10

Oxidation Resistance of Nanocrystalline Alloys

Rajeev Kumar Gupta[1], Nick Birbilis[1] and Jianqiang Zhang[2]
[1]*Department of Materials Engineering, Monash University,*
[2]*School of Materials Science & Engineering, The University of New South Wales, Australia*

1. Introduction

Nanocrystalline (nc) materials are single or multi-phase polycrystalline solids with a grain size of a few nanometers, typically less than 100 nm. Owing to the very fine grain size, the volume fraction of atoms located at grain boundaries or interfaces increases significantly in nanocrystalline materials [1]. A simple geometrical estimation, where the grains are assumed as spheres or cubes, yields the following values for the volume fraction of the interfaces: 50% for 5 nm grains, 30% for 10 nm grains and about 3% for 100 nm grains [2-5]. These values of interface volume fraction are several orders of magnitude higher than those of conventional microcrystalline materials. Consequently, nanocrystalline materials exhibit properties that are significantly different from and often improved over, their conventional microcrystalline (mc) counterparts. For example, nanocrystalline materials exhibit increased mechanical strength [6-10], enhanced diffusivity [11], improved corrosion resistance (some nanocrystalline materials) [12-20], optical, electrical and magnetic properties [21-24]. Due to their unique properties, nanocrystalline materials have attracted considerable research interests and the field of nanocrystalline materials has now become one of major identifiable activities in materials science and engineering.

Metals exposed to high temperature oxygen-containing environments form oxides. If an oxide scale can form and the oxide is dense and adherent, then this scale can function as a barrier isolating the metal from the external corrosive atmosphere. This oxide scale is called protective oxide scale. On the other hand, if a non-protective oxide scale is formed, oxygen can penetrate through the scale and the oxidation will extend further into the metal substrate, causing a rapid metal recession. Of all oxides, chromia and alumina are two kinds of oxides thermodynamically and kinetically feasible to meet the requirement for resisting high temperature oxidation.

Alloys containing aluminium or chromium can be selectively oxidised to form alumina or chromia. To form an external oxide scale, the concentration of aluminium or chromium should reach a critical value. Nanocrystalline alloys promote this selective oxidation process by reducing the critical value. For example, in the conventional microcrystalline Ni-20Cr-Al alloy system, > 6 wt% Al is required to form a protective Al_2O_3 scale at 1000°C [25]. If the Al content is lower than 6 wt%, complex oxide mixtures consisting of Cr_2O_3, $NiCr_2O_4$ and internal Al_2O_3 form, resulting in high reaction rates and poor oxidation resistance. With a nano-crystalline alloy structure, this value can be substantially reduced to 2 wt% Al, when

the grain size is 60 nm [26]. This promotion effect is also evident for the K38G alloy containing 3.5-4 wt% Al and 16% Cr, which forms external Cr_2O_3 scale and internal Al_2O_3 precipitates in the cast form (large grains) but only Al_2O_3 when in the form of sputtered nano-crystalline structure [27-30].

The unique structure and high grain boundary fraction, enhances diffusion of impurities and alloying elements, and changes materials thermodynamic properties [31-33] which are expected to cause a considerable difference in the resistance of nanocrystalline materials to environmental degradation (oxidation) at high temperatures. For practical application of these nanocrystalline materials, an acceptable level of resistance to environmental degradation is required. However, the effect of the nanocrystalline structure on the high-temperature oxidation resistance has attracted only a limited research attention. Oxidation resistance of nanocrystalline Ni-Cr-Al [34-36], Fe-Cr [37-39], and Zr [40-43] based alloys have been mainly investigated and in most of the cases, oxidation resistance has been reported to improve due to nanocrystalline structure.

The properties of oxides (Al_2O_3, SiO_2 or Cr_2O_3) formed during oxidation [44,45,46] also depend upon the grain size of the alloy and nanocrystalline structure alters the properties of oxide. For example, more uniform oxide scale with finer grain size and higher Cr or Al content is formed on the nanocrystalline alloys [34-36]. The oxide scales formed from nanocrystalline materials exhibit enhanced plastic deformation (due to fine grain size of formed oxide), which can release the stresses accumulated in the scales, and therefore the scale spallation tendency is reduced. It was reported that cyclic and long-time oxidation resistance was significantly improved by applying nanocrystalline coatings on type 304 stainless steel [47,48], Ni-Cr-Al [27], Co-Cr-Al [49], and Ni-(Co)-Cr-Al [28-30].

In order to investigate the possible differences in oxidation resistance along with any underlying mechanisms, understanding the nanocrystalline structure of a material is essential. This chapter will therefore first describe the structure of nanocrystalline materials, their thermodynamic properties and the possible effects of changes in the material structure (caused by such fine grain size) that may influence the oxidation resistance of a material.

2. Structure and properties of nanocrystalline alloys

2.1 Dual phase model

The unique properties of nanocrystalline materials are associated with very fine grain size, whereby, depending upon the grain size, interfaces can include up to 50% of the atoms in the material [2-5]. Therefore determination of the structure and associated properties of individual features of a nanocrystalline structure becomes very important. Various models representing the structure of nanocrystalline materials, such as "gas like" model as suggested by Birringer et al. [5] and a "frozen gas like" model suggested later [1,50], are proposed in the literature. However, the structure of nc-materials, in general, may be described as a composition of two components: a crystalline component (CC), which is formed by small equiaxed single crystals each with random crystallographic orientations and the intercrystalline component (IC), which is formed by the interfaces between the crystallites (grain boundaries) and intersection points of these interfaces (triple junctions). The second component may be characterized by the reduced atomic density and inter-atomic spacing deviating from those in the perfect crystal lattice. The IC surrounds the

nanometer-sized crystals and forms a network between them [1,21]. As grain size reduces, the IC increases and it may even exceed CC.

Various researchers support the view of the two phase model of nanocrystalline metals. For example, extended x-ray-adsorption fine structure (EXAFS) and Mössbauer spectroscopy of ball-milled iron indicated the presence of two phases as characterized by significantly different atomic arrangements. These different atomic arrangements can be attributed to the presence of interfacial region and crystalline region [51]. Similarly, EXFAS investigation of nanocrystalline Fe and Pd indicated a large reduction in the atomic coordination number, supporting the idea of a very disordered structure at the interfaces [52-56]. Positron-lifetime spectroscopy measurements showed a large density of vacancy-like defects in grain boundaries and relatively large free volume at the triple points arising from misorientation-induced atomic instability of these sites [57]. Elastic relaxation of the interfaces occurred with a very different parameter than conventional coarse grain size polycrystalline materials. Modelling of thermoplastic properties and structure demonstrates that two phase model is an appropriate mean to account for the vibrational density of states and excess energy density in terms of grain boundary [58]. Similar to experimental findings, computer simulation of nanocrystalline iron has shown that grain boundary component in nanocrystalline material is very high and is a strong function of grain size [59,60].

In discussing the structure of nanocrystalline materials further, the following terminology will be used in the text. Three types of grain contacts are possible in a polycrystalline material. They include, a) contact surfaces, b) contact lines and c) contact points. Surfaces of two grains which contact one another are called as contact interfaces. A contact line may represent a common line for three or more adjacent grains. A contact line of three grains is called triple junction. The boundary of grain is its surfaces. Grain boundaries which are seen in the metallographic slides are the section of interfaces by slide plane. A triple point is a section of triple junction by a plane. A detailed description of the terminology used here can be found elsewhere [61].

2.2 Volume fraction of crystalline and intercrystalline regions

Mutschele and Kirchheim [62] proposed following relation to evaluate the volume fraction (C_{ic}) of nanocrystalline materials associated with intercrystalline regions,

$$C_{ic} = 3\delta / d \tag{1}$$

where, δ is the average grain boundary thickness and d is the average diameter of the grains and grains are considered to be cubes. Later, Palumbo et. al. [2] have shown that equation 1 was not suitable for the calculation of volume associated with triple points and to make it more general (to account for the triple points associated with the intercrystalline component) they proposed following relationship for the calculation of the intercrystalline component (V_t^{ic}):

$$V_t^{ic} = 1 - \left[\frac{d-\delta}{d}\right]^3 \tag{2}$$

where, d is the maximum diameter of an inscribed sphere. This yields the following relation for grain boundary volume fraction (V_t^{gb}),

$$V_t^{gb} = \left[\frac{3\delta(d-\delta)^2}{d^3} \right] \tag{3}$$

The volume fraction associated with triple points (V_t^{tp}) is then given by,

$$V_t^{tp} = V_t^{ic} - V_t^{gb} \tag{4}$$

Using above equations and applying a boundary thickness (δ) of l nm [2, 62,63], the effect of grain size (*d*), in the range of 2 nm to 1000 nm, on the calculated volume fractions corresponding to intercrystalline regions, grain boundaries, and triple junctions, is shown in Figure 1. The intercrystalline component increases from a value of 0.3% (at a grain size of l000 nm) to a maximum value of 87.5% at a 2 nm grain size (Figure 1). The volume fractions associated with intercrystalline regions and perfect crystal are equivalent (i.e., 50%) at a grain size of ~ 5 nm. In assessing the individual elements of the intercrystalline fraction, it is noted that the triple junction volume fraction displays greater grain size dependence than that of the grain boundaries. In the range 100 nm to 2 nm, the triple junction volume fraction increases by three orders of magnitude, while the grain boundary volume fraction increases by little over one order of magnitude. In the nanocrystalline range (i.e., d ~ 10 nm), the grain boundary fraction only increases from ~27% at 10 nm, to a maximum value of ~ 44% at 3 nm. Over the same range of grain sizes, the triple junction fraction increases from ~3% to a value of 50%.

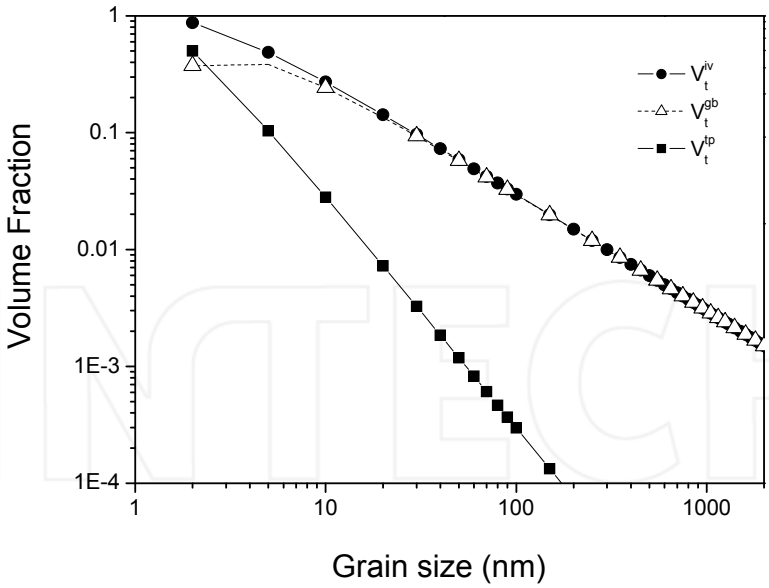

Fig. 1. The effect of grain size on the volume fractions of intercrystalline region, grain boundaries and triple points; calculated from equations 2-5 and assuming the grain boundary thickness to be 1 nm [2].

Based on Figure 1, properties which are influenced by the grain boundary and triple points are expected to be altered significantly when grain size is refined to, or below, 100 nm. The effect of triple points is more pronounced when the grain size is less than 10 nm; consequently material properties with grain size less than 10 nm would be significantly different than those with grain size > 10 nm.

2.3 Thermodynamic properties of nanocrystalline materials

Many researchers have described grain boundaries in nanocrystalline materials as more disordered than those in conventional microcrystalline materials [64-67]. For example, investigations on nanocrystalline Fe have demonstrated that grain boundaries in nanocrystalline Fe differ significantly from the grain boundaries in conventional polycrystalline Fe [64-69]. Thermodynamic properties (specific heat at constant pressure, heat of fusion and stored enthalpy) of ball-milled Fe and other nanocrystalline materials, investigated by Fecht suggested [64-69] that the grain boundaries' energy in nanocrystalline materials to be considerably greater than in the case of equilibrated grain boundaries in microcrystalline materials. In conventional polycrystalline materials, grain boundary energy, as determined by experiments, as well as static and dynamic simulations, is approximately 1 J/m^2, whereas, this value soars to 4 J/m^2 in nanocrystalline materials [70-75].

Significantly different thermodynamic properties of nanocrystalline materials are expected to increase the Gibbs free energy of the materials alloys which can be represented as per following relationship:

$$G= V_t^{gb} .G^{gb}+ V_t^{tp} .G^{tp}+ V_t^{cc} .G^{cc} \quad (5)$$

where, G^{gb}, G^{tp} and G^{cc} are the standard gibbs free energies of grain boundaries, triple points and grains.

Increases in the interfacial energy may lead to a significant increase in the free energy which can be described simply as (neglecting second order contributions due to specific heat differences):

$$\Delta G= \Delta H - T\Delta S \quad (6)$$

Enthalpy difference, ΔH, is shown to be quite higher in nanocrystalline materials than conventional microcrystalline materials. For example it has been shown that ΔH of nanocrystalline Fe increases with decrease in grain size [64-67,76]. Similar behaviour was reported for nanocrystalline copper as well. For example, nanocrystalline Cu, prepared as a powder by vapour deposition followed by compaction releases 300 J/mol at 430K when analysed immediately after compaction and 53 J/mol at 450K when analysed five days after preparation. Such values of enthalpy release have also been confirmed by a study on nanocrystalline Cu prepared by electrodeposition and cold rolling [77-79]. Comparison of these data show that nanocrystalline materials are far from equilibrium, not only because they contain a large amount of interfaces but also because these interfaces are not equilibrated. Therefore, these materials should have high value of free energy which may result in higher reaction rate at the nanocrystalline surfaces.

The total free energy also depends upon entropy term (equation 1), however, evaluation ΔS is not straightforward since there is a little reported in the literature on the entropy contribution from grain boundaries and interfaces for crystals of any size. Although it is expected that this entropy contribution is small and it can also be conceived that non-equilibrated grain boundaries have higher entropy. A value of 0.36 mJ/m^2 K has been estimated for as-prepared nanocrystalline Pt, in contrast to the value for conventional grain boundaries of 0.18 mJ/m^2 K [80]. In fact, the excess entropy per atom sitting in a grain boundary is a substantial part of the entropy of fusion, but the overall entropy per mole of substance sums up to a limited amount even for materials with very small grains. Using this knowledge of enthalpy and entropy, the free energy of nanocrystalline copper has been reported to be higher than that of coarse grain copper [80,81].

2.4 Diffusion in nanocrystalline materials

In general, atomic transport in nanocrystalline materials differs substantially from that in coarse-grained material, due to the crystallite interfaces providing paths of high diffusivity. In conventional microcrystalline materials, crystal volume self-diffusion or substitutional diffusion dominates, at least at temperatures higher than approximately half of the melting temperature. Interface diffusion, in combination with a high fraction of atoms in interfaces, gives rise to modified physical properties of nanocrystalline solids. Furthermore, diffusion processes may control the formation of nanocrystalline materials, for example, by means of crystallization of amorphous precursors, as well as the stability of nanocrystalline materials (relaxation, crystallite growth), their reactivity, corrosion behaviour, or interaction with gases. The relevance of diffusion-controlled processes demands a comprehensive understanding of atomic diffusion in nanocrystalline materials. Detailed discussion of the diffusion processes in the nanocrystalline material is out of the scope. For the readers interest it could be found elsewhere [82-85]. A recent study on nanocrystalline Fe has shown that the diffusion coefficient of Cr in Fe can be enhanced by several orders of magnitude by reducing the grain size to nanometer level [11].

Diffusion in a material can be expressed as the combined effect of diffusion through the grain boundaries and lattice diffusion and can be written as:

$$D_B = fD_{gb} + (1-f)D_b \rightarrow D_B = f\left(D_{gb} - D_b\right) + D_b \tag{7}$$

where, f is the grain boundary fraction, D_{gb} is the grain boundary diffusion coefficient and D_b is the bulk diffusion coefficient of B in the alloy. Assuming the cubic shape of grains, the grain boundary area fraction (f) can be calculated as per equation (1). Because D_{gb} is much larger than D_b, the effective diffusion coefficient of nanomaterials increases significantly by their high area proportion of grain boundaries.

3. Factors effecting the oxidation behavior of a nanocrystalline alloy

An effective protection of metallic materials against high temperature oxidation is based on the protective oxide scale which acts as diffusion barrier, isolating the material from the aggressive atmosphere. The principle is simple, however its application is complex; to act as a real barrier the oxide film needs to be dense and homogenous and has to cover entire

surface of the alloy. Oxide scale should possess mechanical properties as close possible to the base material and most importantly it should be adherent to the substrate even in the presence of large thermal shocks. These parameters largely depend upon the alloy composition and microstructure and can be optimized choosing the right combination of the two. The development of the nanocrystalline structure has provided a large scope of modification of the microstructure and to investigate the effect of nanocrystalline structure on the properties of oxide scale formed and therefore the resultant oxidation resistance. Since nanocrystalline materials are thought to be very reactive due to presence of large fraction of defects, it was supposed that they may possess poor oxidation resistance. Here both the possibilities of improvement and deterioration of oxidation resistance due to a nanocrystalline structure are discussed:

3.1 Deterioration of oxidation resistance caused by nanocrystalline structure

The following are possibilities which may lead to a higher oxidation rate in a nanocrystalline structure:

1. It was described in the previous section that free energy of a nanocrystalline alloy is increased as the atoms residing at the grain boundaries are more reactive than the atoms at grains. This increased free energy of nanocrystalline materials would accelerate the reactions occurring upon them and therefore oxidation rate of nanocrystalline structure is expected to increase, leading to poor resistance to environmental degradation.
2. Increase in oxide nucleation sites and, therefore, formation of oxide scale with comparatively finer grain size through which diffusion of oxygen and metal would be faster because of enhanced diffusion through the grain boundaries. Such phenomenon occurring in Ni-Cr-Al alloy accelerates diffusion of Al through the oxide which facilitates the formation of Al oxide [34] and leads to substantial improvement in oxidation resistance. However, such diffusion in a pure metal may lead to a significant higher oxidation rate if a non-protective oxide scale forms. For example in cause of pure Ni, nanocrystalline structure has reported to increase the oxidation rate because of increased diffusion of Ni and oxygen through the grain boundaries of oxide formed on the metal [86].
3. In the case of alloys where the concentration of solute atoms is lower than a critical value for external oxide scale formation, internal oxidation occurs. The oxidation rate is enhanced because of increased diffusivity of oxygen through grain boundaries leading to severe internal oxidation near the surface. Rapid oxidation occurs for these alloys.

3.2 Improvement in oxidation resistance caused by the nanocrystalline structure

Improvement in oxidation resistance of some engineering alloys where protective oxide scales are formed at high temperatures is noticed in their nanocrystalline forms. Improved oxidation resistance of FeBSi [87], Ni-based alloys [88-93], Zr and its alloys [40-43], Cr-33Nb [94], Fe-Co based alloys [95,96] and Cu-Ni-Cr alloys [97] is reported in their nanocrystalline form (in comparison to their microcrystalline counterparts). The mechanistic role of a nanocrystalline structure leading to the improved oxidation resistance is discussed below:

3.2.1 Enhanced diffusivity and oxidation resistance

Certain alloys can develop a continuous layer of the protective oxide of more reactive alloying elements which forms basis for the development of oxidation resistanct alloys. Such alloys are Fe, Ni, Co based, with Al, Cr or Si as the reactive alloying additives. For example, Iron-chromium alloys (such as stainless steels) are the most commonly employed oxidation resistant materials. It has been established that when time-dependent inward flux of oxygen is less than the time-dependent outward flux of solute (Cr), a continuous layer of Cr-oxide is formed at or very near the surface. Formation of such oxide layer and therefore oxidation resistance of Fe-Cr alloys depend upon the supply of solute from the alloy to alloy/oxide scale. It was established in the literature that a fine grain (~17 μm or less) stainless steel easily developed a uniform layer of Cr_2O_3. For an alloy with grain sizes greater than ~40 μm, this protective layer of Cr_2O_3 was difficult to form due to insufficient grain boundary diffusion and inadequate chromium supply [98-100]. In nanocrystalline materials where grain size is very fine and diffusion coefficients are high, such Cr oxide formation should be facilitated by a large extent. Since enhanced diffusion of alloying elements in the nanocrystalline structure facilitates the formation of protective oxides, therefore alumina, chromia and/or silica forming alloys should have improved oxidation resistance in their nanocrystalline form.

3.2.2 Nucleation sites and lateral growth of passive film

In most alloys, nucleation and growth are the mechanism of oxide scale formation during oxidation [44,45,101-103]. It is widely reported that nucleation of oxide is favoured at the high energy sites, i.e., surface defects in the form of dislocations, grain boundaries, triple points, impurities etc. Since nanocrystalline materials are composed of the large fraction of surface defects therefore they offer a large fraction of closely spaced nucleation sites. During the lateral growth of oxide, these nucleation sites become very important as the presence of closely spaced nucleation sites reduces the lateral distance necessary for the lateral growth of a uniform oxide layer to cover the entire surface.

Lobb and Evans [104] have reported an improvement in the oxidation resistance of fine grained conventional microcrystalline materials as a result of increased grain boundary area fraction as the grain boundaries acts as the preferential nucleation sites for Cr_2O_3. They reported that the oxide film nucleated at the grain boundaries needs to grow laterally for the formation of a uniform oxide layer and reported that the finer the grain size, the better the uniformity of oxide should be. Later it was shown that above a critical grain size, formation of a uniform Cr layer was not possible which could be understood based on the combined role of diffusion and nucleation site densities in the alloys [44,45,98-100]. However, these studies were performed on the material where minimum grain size was a few microns. Nanocrystalline materials offer a huge amount of nucleation sites. Therefore, formation of a homogenous compact layer able to cover whole surface is facilitated, which is expected to result in a significant improvement in the oxidation resistance.

3.2.3 Structure of the oxide scale

Mechanical properties, microstructure, adhesion and growth of oxide scale has been reviewed recently [105,106] and it has been found that oxidation resistance of a metal largely

depends upon their physical properties (e.g., crystal size, morphology and crystallographic orientation of oxides formed, lattice mismatch with the base metal, adhesion of oxide layer) of oxide [105,106]. For example, fine grained oxide scales often show a fast creep rate at high temperatures, releasing the stresses accumulated in the scales and, therefore, decrease in scale spallation tendency. This may have important implication in reducing the spallation of oxides at high temperature. Since nanocrystalline materials provide several orders of magnitude more nucleation sites than the microcrystalline materials therefore grain size of the oxide developed on nanocrystalline materials is expected to be finer. This finer grain size of oxide suppresses oxide scale spallation in nanocrystalline form. This effect has been demonstrated in high temperature oxidation tests of several nanocrystalline alloys [27-30,47].

It was also proposed that fine nano-sized oxide structure reduces conductivity which suppresses the transport of the oxidizing species, enhancing oxidation resistance. This proposal was successfully used to explain improved oxidation resistance of Zr and Zr based alloys [107]. However, it is not clear if this model also applies for other alloys.

It is important to note that the above factors can operate both indifferently and in combination [12]. The nature of the influence of nanostructure on the diffusion-assisted corrosion (viz., high temperature oxidation) depends on the role of the predominantly diffusing species in a given alloy. For example, oxidation resistances of an iron-aluminide and an Fe-B-Si alloy in the nanocrystalline state are reported to be superior to that in their microcrystalline state [87,108]. This behaviour is attributed to Al and Si, the well-known protective oxide film formers, being the predominantly diffusing species respectively in the two alloys, and the nanostructure facilitating their diffusion and expedited formation of protective films (of Al/Si oxide). Therefore, it is important to consider all the factors effecting the oxidation resistant, and the net effect of all the parameters would determine the change in the oxidation rate caused by nanocrystalline structure.

4. Critical concentration of solute required for the transformation of internal to external oxidation as a function of grain size

Oxidation of engineering alloys is very complex as the components of the alloys has different affinities for the oxygen, and reacting atoms do not diffuse at the same rates in the oxides or alloy substrates. Various types of oxides can be formed on and in the alloy. Atomic ratios of the elements in the oxide scale may differ significantly from those in the alloy. When oxygen and metal atoms diffuse and react at the surface of an alloy, an external oxide layer is formed on the surface and this is termed as the “external oxidation”. For external oxidation, outward flow of metal atoms must exceed the inward flow of oxygen, whereas, when inward flow of oxygen exceeds the outward flow of the metal atoms, oxygen diffuses inside the metal and oxidation takes places within the alloy. This process is termed as “internal oxidation” which leads to catastrophic loss in the material property [44,45,109]. Figures 2 and 3 schematically show internal and external oxidation for alloy A-B under the conditions where only B oxidises and both A and B oxidise, respectively.

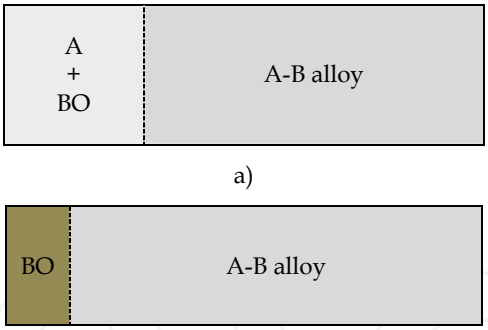

Fig. 2. Wagner's model of the transition from the internal to external oxidation of alloy A-B under the condition where only B can oxidize: a) B is less than the critical amount of B required for the transition and b) B is higher than the critical content of B required for the transition from the internal to external oxidation [44,45, 110-112].

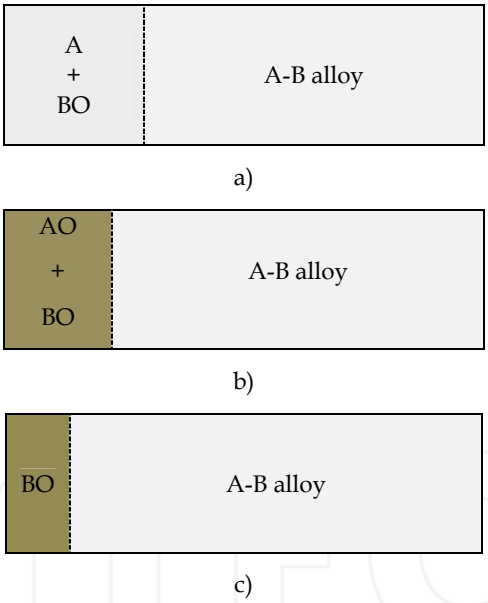

Fig. 3. Wagner's model of the transition from the internal to external oxidation of alloy A-B under the condition where both A and B can oxidize: transition from internal oxide (a) to external composite oxide scale (b) to external exclusive oxide scale (c) [44,45,110-112].

From a kinetic point of view, there is a minimum concentration of oxide former required to ensure that the alloy chromium (or any other oxide former) diffusion flux must be sufficient to outweigh inward oxygen diffusion, thus favouring external scale growth over internal oxide precipitation. The required concentration, $N_M(Crit)$, is found from Wagner's analysis [45,110-112] to be:

$$N_B(Crit1) = \left(\frac{g.\pi}{3} \cdot \frac{V_{AB}}{V_{BO_\nu}} \cdot \frac{N_O^{(s)} D_O}{D_B}\right)^{1/2} \quad (8)$$

Here $N_O^{(s)} D_O$ is the oxygen permeability in the alloy matrix, V_{AB}, V_{BO_ν} are the molar volumes of alloy and oxide, D_B is the diffusion coefficient of chromium or aluminium in the alloy, and g the critical volume fraction of oxide required to form a continuous layer. According to this equation, the critical value for external chromia formation in Ni-Cr at 1000°C is N_{Cr} = 0.29 and for alumina formation in Ni-Al at 1200°C is N_{Al} = 0.11 [45], both in agreement with the experimental measurements. The requirement for these relatively large concentrations of Cr or Al to form a complete protective scale will, in many cases, change other alloy properties, which limits the applicability of this approach, particularly at lower temperatures.

No sooner has the continuous scale of chromia or alumina become established than the steady-state growth of this oxide starts. For chromia/alumina scale growth to be maintained, an alloy must supply chromium/aluminium by diffusion from its interior at a rate sufficient to balance the rate at which the metal is consumed in forming new oxide. Wagner's diffusional analysis [112] leads to the requirement:

$$N_B(Crit2) = \frac{V_{AB}}{V_{BO_\nu}} \left(\frac{\pi k_p}{2D_B}\right)^{1/2} \quad (9)$$

where V_{AB}, V_{BO_ν} are the molar volumes of alloy and oxide, k_p is the parabolic rate constant for scale thickening:

$$x^2 = 2k_p t \quad (10)$$

with x the scale thickness formed in time, t, and D_B the alloy interdiffusion coefficient. The quantity $N_B(Crit2)$ is the minimum original alloy chromium concentration necessary to supply metal to the alloy-scale interface fast enough to support exclusive chromia scale growth.

To avoid internal oxidation and maintain external chromia/alumina scale, the concentration of aluminium/chromium should be higher than both N_B(Crit1) and N_B(Crit2). In nanocrystalline materials, D_B could be very high [11,12] according to Eqn 6, and therefore both N_B(Crit1) and N_B(Crit2) decrease significantly which will lead to substantial increase in the formation of a protective alumina/chromia external scale, therefore increased oxidation resistance. Assuming the alloy grains are cubic, the area proportion of grain boundary f can be calculated f=2δ/d. Also considering Dgb>>Db, Eqn 7 can be simplified as [113]:

$$N_B(Crit1) = A\left(D_b + \frac{2\delta}{d} D_{gb}\right)^{-1/2} \quad (11)$$

where

$$A = \left(\frac{g\pi N_O^{(s)} D_O V_{AB}}{2V_{BO_\nu}}\right)^{1/2},$$

thus reduction in grain size results in the reduction of N_B(Crit1).

Using Equations (1) and (6), the critical concentration N_B(Crit2) is calculated as:

$$N_B(crit2) = B.\left(D_b + \frac{2\delta}{d}D_{gb} - \frac{2\delta}{d}D_b\right)^{-\frac{1}{2}} = B\left(\frac{\sqrt{d}}{\sqrt{2\delta(D_{gb}-D_b)+d.D_b}}\right) \quad (12)$$

Where,

$$B=\frac{V_{AB}}{V_{BO_v}}\left(\frac{\pi k_p}{2}\right)^{1/2}.$$

At a given temperature and external oxygen partial pressure, N_B (crit1) and N_B (crit2) are a function of only grain size *(d)* of the alloy, diffusion coefficients (D_{gb} and D_b) and grain boundary width (δ) of the alloy.

The critical concentration of B required, where only bulk diffusion can control the oxidation (i.e., the area fraction of grain boundary is very small such that $D=D_b$), can be calculated as:

$$N_{oB}(crit2) = B.(D_b)^{-\frac{1}{2}} \text{ and } N_{oB}(crit1) = A.(D_b)^{-\frac{1}{2}} \quad (13)$$

From equations (10), (11) and (12), for an alloy of grain size, d, the ratio *(X)*, critical concentration of B required for external oxidation in material with a grain size d to that when the bulk diffusion coefficient dominates, can be given as:

$$X = \frac{N_B(crit1)}{N_{oB}(crit1)} = \frac{N_B(crit2)}{N_{oB}(crit2)} = \sqrt{\frac{d}{2\delta\left(\frac{D_{gb}}{D_b}-1\right)+d}} = \sqrt{\frac{1}{f\left(\frac{D_{gb}}{D_b}-1\right)+1}} \quad (14)$$

Since, the values of D_{gb} and D_b are available from the literature, the value of X can be calculated as a function of grain size, time and temperature. Above relationship may be very useful in comparing the change in the critical amount of B (Al or Cr) caused by nanocrystalline structure at a given temperature.

Given that the critical amount of B (N_B(crit1)) required for a material with grain size d_0 is w, according to equation (13), the ratio for the critical amount of B required for a grain size of d to that for the grain size d_0 can be expressed as X':

$$X' = \frac{N_B}{w} = \sqrt{\frac{d(2\delta(D_{gb}-D_b)+d_0.D_b)}{d_0(2\delta(D_{gb}-D_b)+d.D_b)}} \quad (15)$$

For Fe-Cr alloy, X′ is calculated based on available data listed in the Table 1 (extrapolated from the literature [114,115] with d_0 assumed to be 5 micron, and plotted it as a function of grain size in Fig 4. Figure 4 clearly shows that Cr required for such transition decreases substantially when grain size is below 100 nm.

Temperature	Lattice (D_b) m^2/s	GB (D_{gb}) m^2/s
300 °C	1.2×10^{-26}	8.6×10^{-22}
840°C	1.5×10^{-15}	3.7×10^{-12}

Table 1. Diffusion coefficients of Cr in Fe-Cr alloy [114,115]

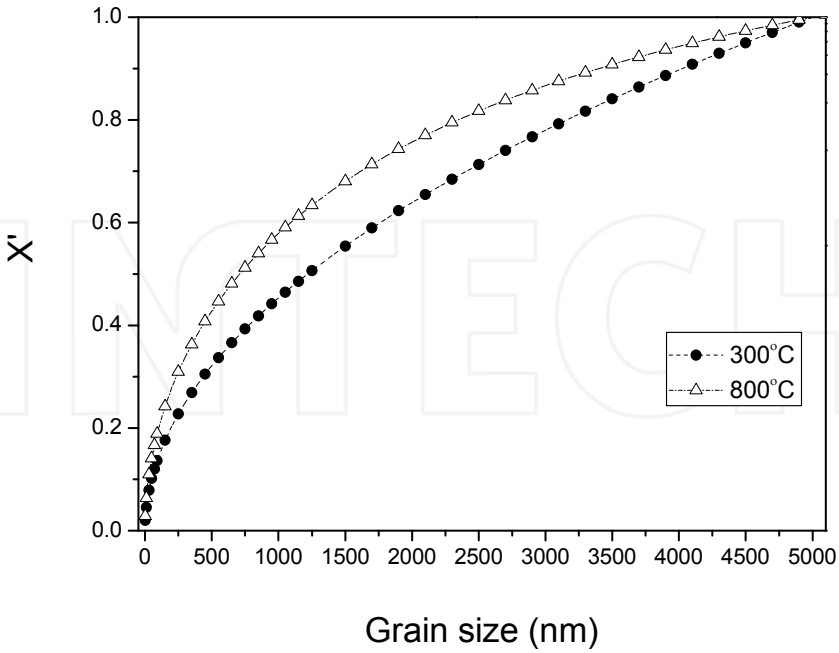

Fig. 4. Plot of the grain size with X′ (ratio of critical amount of Cr required for external passive oxide layer formation in a Fe-Cr alloy of grain size d to critical amount of Cr required for such transition in a Fe-Cr alloy with a grain size of 5 μm) [12,39].

5. Oxidation resistance of nanocrystalline alloys – Some examples

5.1 Fe-Cr alloys

5.1.1 Oxidation resistance of nanocrystalline and microcrystalline Fe-10Cr alloys

The oxidation behaviour of Fe-Cr alloys have been extensively investigated in the literature and reviewed by Wood [102]. Fe-Cr alloys are known for their high oxidation resistance due to formation of a Cr rich oxide layer which largely depends upon the selective oxidation of Cr. As already demonstrated before, a nanocrystalline structure is expected to cause a significant reduction in the Cr concentration required for chromia scale formation. For the validation of this hypothesis various nanocrystalline and microcrystalline Fe-10Cr and Fe-20Cr alloys were prepared by high energy ball milling followed by compaction and sintering which are described elsewhere [116]. The oxidation behaviour of such Fe-Cr alloys was investigated in a temperature range of 300 to 400°C by continuous weight gain experiments. The experimental details can be found elsewhere [12,38,39].

Weight gain curves representing the oxidation kinetics of nanocrystalline and microcrystalline Fe10Cr alloys, in the temperature range of 300-400°C are presented in

Figures 5-7 [12,38,39]. Oxidation kinetics at 300°C shows the microcrystalline alloy to be oxidizing at a considerably greater rate than the nanocrystalline alloy. After 3120 minutes of oxidation, weight gain of microcrystalline Fe-10Cr alloy was found to be nearly seven times greater than that of nanocrystalline alloy of same chemical composition.

Besides the considerably higher weight gain of the microcrystalline alloy, the evolution of oxidation kinetics was also different. Both nanocrystalline and microcrystalline Fe10Cr alloys follow parabolic kinetics for the first 240 minutes of oxidation (as evident in the weight-gain^2 versus time plot in Figures 5b and 6b). However during subsequent oxidation, nanocrystalline Fe10Cr alloy show considerable deviation from the parabolic behaviour whereas, microcrystalline alloy of same chemical composition continued to follow the parabolic kinetics (Figures 5c and 6c). The marked deviation of the nanocrystalline Fe-10Cr alloy from the parabolic behaviour is accounted for the insignificant increase in the weight-gain of this material after the first 240 minutes of oxidation (Figures 5a, 6a, 5b and 6c). This behaviour could be attributed to some critical change in the chemical characteristic of the oxide scale formed on both nanocrystalline and microcrystalline alloys before and after 240 minutes of oxidation which was described by Gupta et al using SIMS [12,38,39] analysis of oxide formed during various period of oxidation.

Oxidation kinetics of nanocrystalline and microcrystalline Fe-10Cr alloys at 350 and 400°C are presented in Figures 6 and 7. The trend of greater oxidation rate of the microcrystalline alloy, as seen at 300°C is also followed at the two higher temperatures. However, the influence of nanocrystalline structure in improving the oxidation resistance was extraordinarily enhanced at these higher temperatures as indicated by the comparative weight gains after 3120 minutes of oxidation: weight gain of microcrystalline Fe-10Cr alloy was found to be 18 times greater than that of the nanocrystalline Fe-10Cr alloy at 350°C, and nearly 17 times greater at 400°C.

A close observation of the data as presented in Figures 5-7 show that both nanocrystalline and microcrystalline Fe-10Cr alloys follow parabolic kinetics ,i.e., (weight grain per unit area)^2 = kt. The rate constants (k) in nanocrystalline alloy changes with time (Table 2). Oxidation kinetics of nanocrystalline Fe-10Cr can be divided in the two stages, each stage characterized by a unique k value (Table 2). Microcrystalline alloy, on the other hand follow a single parabolic rate constant. As presented in the Table 2, k value for microcrystalline (mc) Fe10Cr alloys are more than an order of magnitude greater than either of the k values for nanocrystalline (nc) Fe10Cr alloy at the three temperatures.

	nanocrystalline Fe10Cr	microcrystalline Fe10Cr
300°C	5.65×10^{-13} (1st stage) and 7.42×10^{-14} (2nd stage)	7.74×10^{-12}
350°C	1.04×10^{-12} (1st stage) and 1.7×10^{-13} (2nd stage)	1.46×10^{-10}
400°C	1.34×10^{-12} (1st stage) and 5.69×10^{-13}(2nd stage)	2.53×10^{-10}

Table 2. Parabolic oxidation rate constants (k) values in $g^2cm^{-4}s^{-1}$[12]

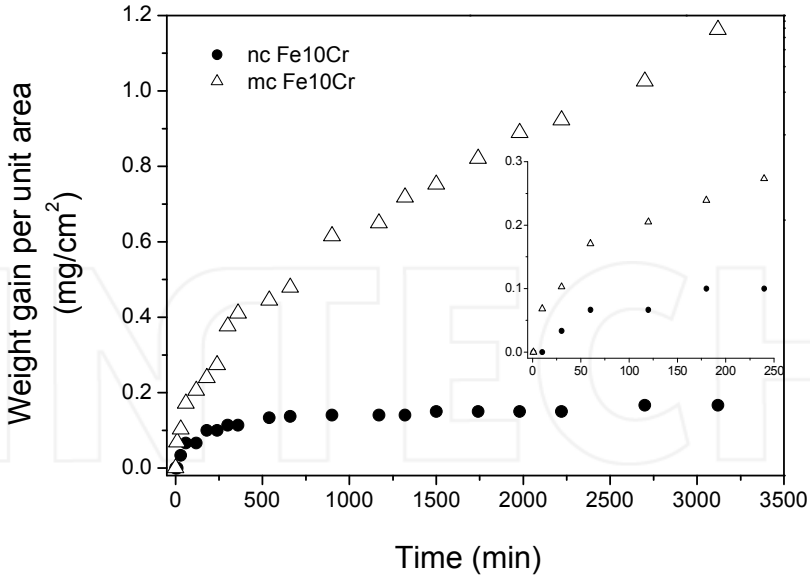

Fig. 5a. Oxidation kinetics of nanocrystalline (nc) and microcrystalline (mc) Fe-10Cr alloys at 300°C as represented by weight-gain vs time plots for 3120 minutes [12,37,39]. Inset shows the zoom of the region representing initial periods of oxidation (up to 240 minutes of oxidation).

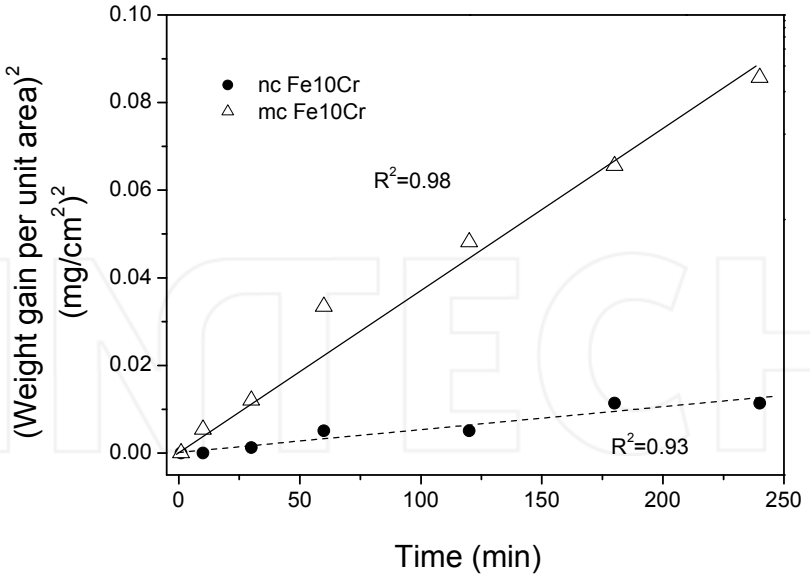

Fig. 5b. Oxidation kinetics of nanocrystalline (nc) and microcrystalline (mc) Fe-10Cr alloys oxidised at 300°C: weight-gain^2 with time (up to 240 minutes) suggesting parabolic kinetics for both mc and nc alloys [12,37,39]

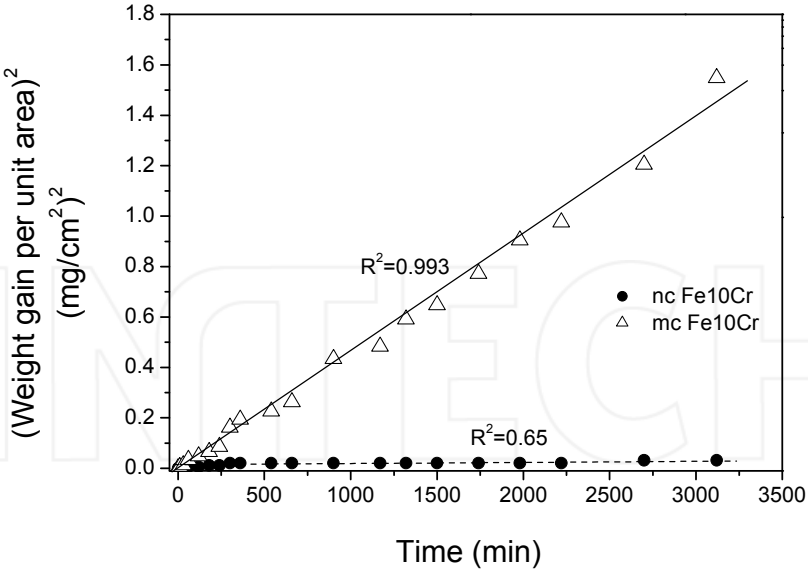

Fig. 5c. Oxidation kinetics of nanocrystalline (nc) and microcrystalline (mc) Fe-10Cr alloys, oxidised at 300°C: weight-gain^2 with time, suggesting parabolic kinetics for mc alloy but departure from parabolic kinetics for nc alloy [12,37,39].

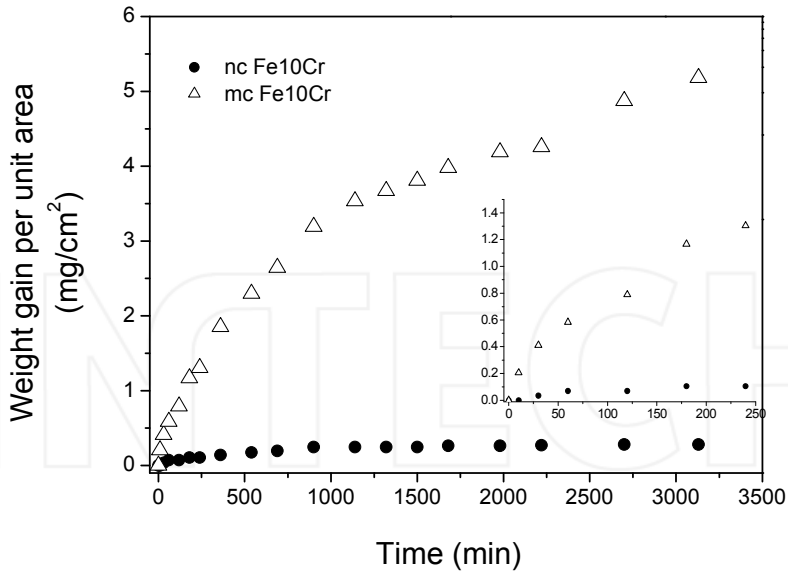

Fig. 6a. Oxidation kinetics (weight-gain vs time plot) of nanocrystalline (nc) and microcrystalline (mc) Fe-10Cr alloys, during oxidation at 350°C for 3120 min in air [12,39]. Inset shows the zoom of the region showing initial periods of oxidation (up to 240 minutes of oxidation).

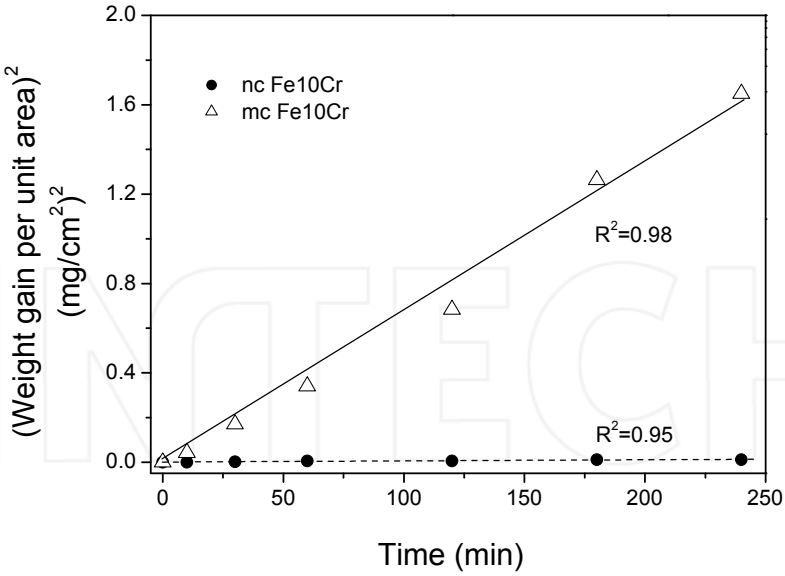

Fig. 6b. Oxidation kinetics of nanocrystalline (nc) and microcrystalline (mc) Fe-10Cr alloys oxidised at 350°C: weight-gain^2 with time (up to 240 minutes) suggesting parabolic kinetics for both mc and nc alloys [12,39]

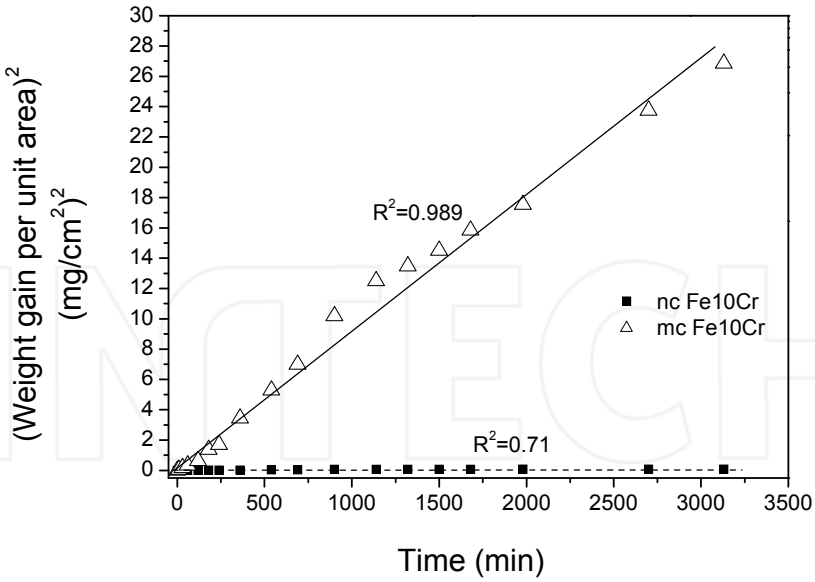

Fig. 6c. Oxidation kinetics of nanocrystalline (nc) and microcrystalline (mc) Fe-10Cr alloys, oxidised at 350°C: weight-gain^2 with time, suggesting parabolic kinetics for mc alloy but departure from parabolic kinetics for nc alloy [12,39].

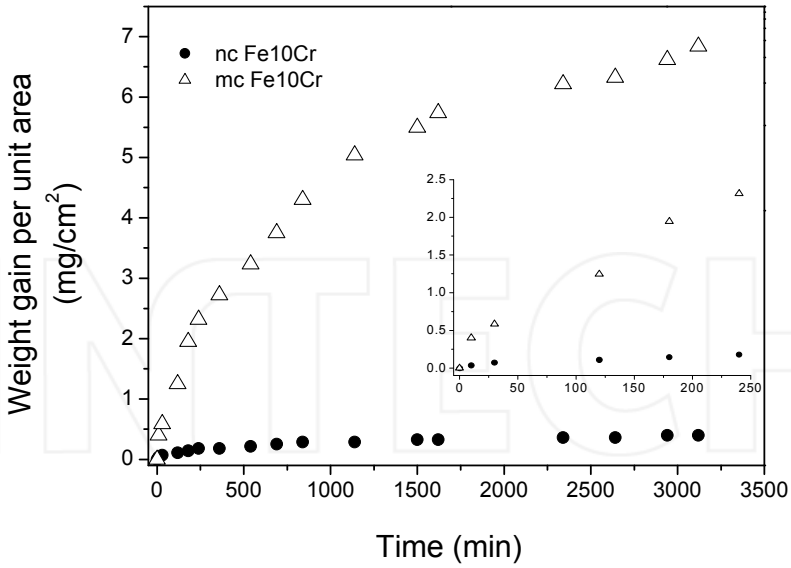

Fig. 7. Oxidation kinetics (weight-gain vs time plot) of nanocrystalline (nc) and microcrystalline (mc) Fe-10Cr alloys, during oxidation at 400°C for 3120 min in air [12,39]. Inset shows a zoom of the region of initial periods of oxidation (up to 240 minutes of oxidation).

5.1.2 SIMS depth profile of oxidized Fe-10Cr alloys

In order to understand the mechanism of improved oxidation resistance of nanocrystalline Fe-10Cr alloy, the composition, including Cr content of the thin oxide films developed on the nanocrystalline and microcrystalline alloys was characterized. The thin oxide films formed over nanocrystalline Fe-10Cr and microcrystalline Fe-10wt%Cr alloys at 300, 350 and 400°C in air were characterised by SIMS depth profiling [12,39].

Oxidation resistance of Fe-Cr alloys was associated the development of a protective layer of Cr_2O_3. Depth profiles for Cr, O and Fe for the nanocrystalline and microcrystalline Fe-10Cr alloys oxidized at the three temperatures for 30, 120 and 3120 min were obtained [12,32,33]. It was found that the oxide film developed on microcrystalline Fe-10Cr alloy is considerably thicker than that on nanocrystalline Fe-10Cr alloy at the three test temperatures [12,39].

The most relevant findings of the SIMS analyses as reported in the literature [12,38,39] are the depth profiles of chromium and their consistency with the trends of oxidation kinetics. The Cr depth profiles obtained after 52 hours of oxidation are presented in the Figures 8-10. At each of the oxidation temperatures, Cr content of the inner layer of nanocrystalline Fe-10Cr alloy was invariably found to be considerably higher than the highest Cr content in the inner layer of microcrystalline Fe-10Cr alloy. This provides an explanation for the greater oxidation resistance of the nanocrystalline Fe-10Cr alloy (as shown in Figures 8-10), since oxidation resistance of Fe-Cr alloys is governed primarily by the Cr content of the thin oxide scale.

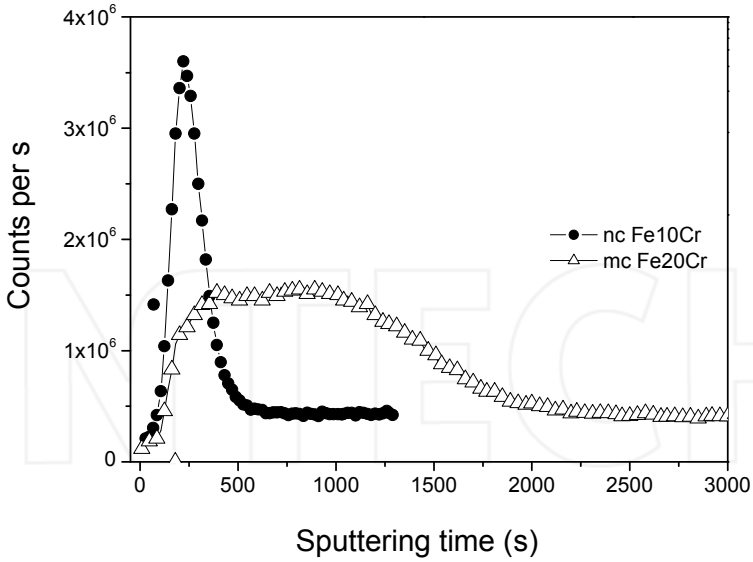

Fig. 8. SIMS depth profiles for Cr the in the oxide scale developed during oxidation of nanocrystalline (nc) and microcrystalline (mc) Fe-10Cr alloys at 300°C for in air for 3120 minutes, using a Cameca ims (5f) dynamic SIMS instrument. SIMS parameters were: Cs^+ ion primary beam (10 nA), depth profiling of craters of 250 μm × 250 μm area [12,39].

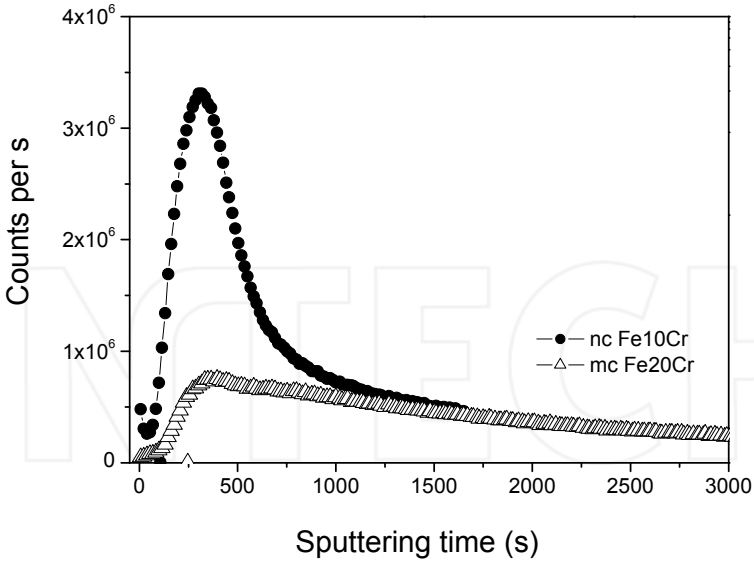

Fig. 9. SIMS depth profiles for Cr the in the oxide scale developed during oxidation of nanocrystalline (nc) and microcrystalline (mc) Fe-10Cr alloys at 350°C for in air for 3120 min, using a Cameca ims (5f) dynamic SIMS instrument. SIMS parameters were: Cs^+ ion primary beam (10 nA), depth profiling of craters of 250 μm × 250 μm area [12,39].

SIMS analysis as carried out in our previous work [12,39] provides a qualitative analysis of Cr enrichment of the surface. Based on such qualitative analysis of Cr content, a Cr_2O_3 oxide layer was proposed to develop in nanocrystalline alloy, whereas, it was proposed that a mixed Fe-Cr oxide layer forms in case of microcrystalline alloy. A Future study quantifying the Cr, Fe and O contents of oxide layer and their oxidation states using techniques such as X-ray photoelectron spectroscopy (XPS) must provide a better understanding of the effect of nanocrystalline structure on the chemical composition of oxide layer.

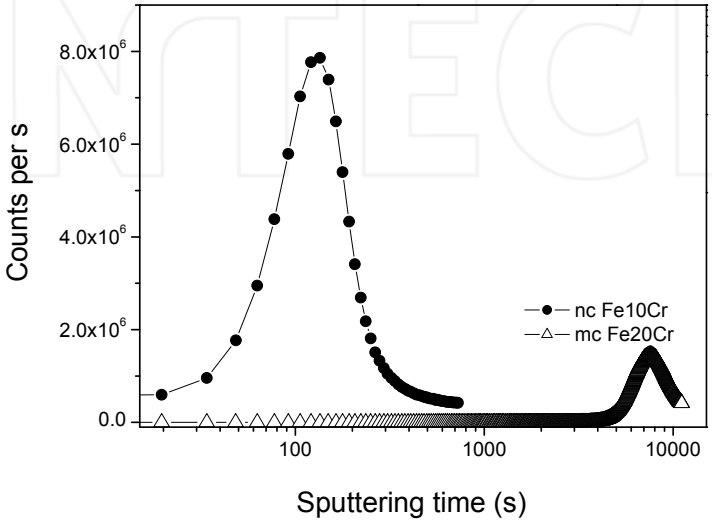

Fig. 10. SIMS depth profiles for Cr the in the oxide scale developed during oxidation of nanocrystalline (nc) and microcrystalline (mc) Fe-10Cr alloys at 400°C for in air for 3120 min, using a Cameca ims (5f) dynamic SIMS instrument. SIMS parameters were: Cs^+ ion primary beam (10 nA), depth profiling of craters of 250 μm × 250 μm area [12,39].

5.1.3 Oxidation resistance of nanocrystalline Fe10Cr versus oxidation of microcrystalline Fe20Cr alloy

For developing an understanding of how the considerably greater oxidation resistance of nanocrystalline Fe-10Cr alloy (in comparison with microcrystalline Fe-10Cr alloy) compares with the resistance of an alloy with much higher Cr content, samples of microcrystalline Fe-20Cr alloys were also oxidized at 350 °C for durations up to 3120 minutes [12,39]. However, what is most relevant to note is that the weight gain at the end of 3120 minutes of oxidation of microcrystalline Fe-20Cr alloy is similar to that of the nanocrystalline Fe-10Cr alloy at 350 °C for same period of time (shown in Figure 11), suggesting the degree of oxidation resistance conferred due to nanocrystalline structure at only 10% chromium to be similar to that of the alloy with 20% chromium but microcrystalline structure. This finding may have wide industrial applications in developing steel with low Cr but very high oxidation resistance as exhibited by Fe20Cr alloy.

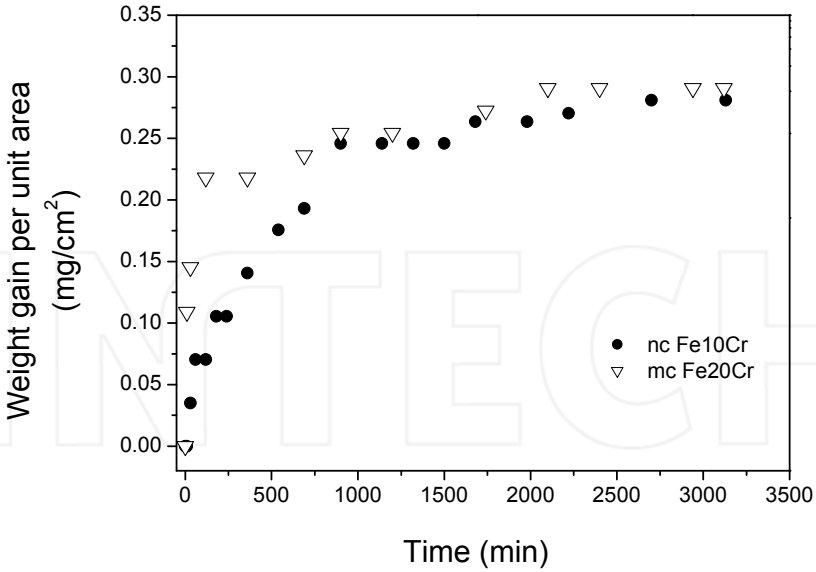

Fig. 11. Comparison of oxidation resistance of nanocrystalline Fe10Cr alloy with that of microcrystalline Fe20Cr alloy at 350°C in air [12,39].

5.2 Ni-Cr-Al based alloys

Oxidation resistance of Ni-Cr-Al based alloys largely depend upon the chemical and physical properties of alumina scale formed during high temperature oxidation. Most of the Ni-Cr-Al alloy contains enough Cr to form external Cr_2O_3 scale but for the application over 1000°C, the chromia scale does not provide any beneficial effect due to the volatilisation problems. Formation of a compact protective Al_2O_3 scale is most efficient in protecting material from the high temperature oxidation. In general, a conventional Ni-20Cr-Al system requires more than 6 wt% of Al to form protective oxide scale which largely depends upon the a) diffusion coefficient of the Al from the bulk to alloy/oxide interface and b) diffusion of Al in the formed oxide scale [45,118].

Since nanocrystalline materials possess significantly higher diffusion coefficient caused by higher fraction of grain boundaries therefore Al required for formation an exclusive Al oxide film can be reduced significantly and nanocrystalline materials should show improved oxidation resistance [88-93,119]. Wang et al [119] were among first researchers to investigate the oxidation resistance of nanocrystalline Ni-Al-Cr alloys and reported a significant improvement in the oxidation resistance of NiCrAl alloys due to nanocrystalline structure. Later, various authors have investigated the oxidation resistance of nanocrystalline NiCrAl alloys with various Al and Cr contents and produced by different methods but in all the cases nanocrystalline structures was reported to enhance the oxidation resistance. Most comprehensive work showing effect of the nanocrystalline structure on NiCrAl alloys was that of Gao et al [88] who reported excellent oxidation behaviour of a nanocrystalline coating of Ni20CrAl alloy over its microcrystalline

counterpart. They reported a coating with grain size less than 70 nm may increase the oxidation rate by 4 times. Increment in oxidation resistance due to grain refinement was more pronounced when grain size was below 100 nm. It has been shown than Al content required to prevent external oxidation can be reduced from 6% to only 2% by reducing the grain size to ~ 60 nm [88-93]. These findings may have large industrial implications as it would provide an opportunity to achieve the desired oxidation resistance with lower Al content.

6. Challenges for application of nanocrystalline alloys at high temperature

For high temperature application, a major problem is thermal stability of the nanocrystalline structure. Thermodynamically, such fine structures could not survive for long times at high temperatures because of the large specific surface energy (driving force) for grain growth. An effective way to prevent this grain growth is by introducing stable second-phase particles in the microstructure, where they play a particle pinning effect (Zener effect) on grain growth [120]. Surprisingly, the coarsening kinetics for nanocrystalline alloys prepared by sputtering is rather slow even without apparent second-phase particles in the microstructure. Lou et al. [19] found that after 100 h oxidation in air at 1000°C, the grains of a sputtered K38G nanocrystalline coating were somewhat coarsened, but still rather fine-grained, growing from 20-100 nm to 200-1000 nm. It is not clear if this high stability against grain growth comes from grain boundary segregation of alloy elements (e.g. K38G alloy contains 3.6% Ti, 1.7% Mo, 2.6% W, 1.7% Ta in the Ni-Cr-Al base), which anchor or retard the grain boundary movement (similar to Zener effect) although no particle formation was apparent, or from the sputtered coating structure itself (columnar structure). Unfortunately, no systematic investigation of temperature and alloy composition effects on the thermal stability of these nanocrystalline alloys is available to date, future research should be carried out for high temperature application of nanocrystallline alloys.

Another problem limiting the application of nanocrystalline materials is preparation of nanocrystalline alloys. Currently, the bulk metallic nanomaterials can only be prepared at the laboratory scale, usually by compacting prepared nanocrystalline powders. However, consolidation of the nanopowders into bulk materials needs high temperature and pressure which may considerably coarsen the structure. Because of this difficulty, surface nanocoating has been considered a potential industry application. Nanocrystalline costing are often prepared by chemical vapour deposition (CVD), physical vapour deposition (PVD), electrochemical deposition, electro-spark deposition, and laser and electron beam surface treatment.

7. Future research

All studies reporting excellent oxidation resistance of nanocrystalline NiCrAl alloys were conducted at high temperatures. However, the grain growth behaviour of the alloys at these elevated temperatures was not determined and therefore many questions remain unanswered. Detailed studies investigating the effect of such fine grain size on the oxide scale formation along with grain growth of material will be helpful in understanding the underlying mechanism of the improved oxidation resistance.

Oxidation behaviour of Fe-Cr alloys as described in the section 5.1 was investigated at moderate temperatures [12,37-39]. Choice of moderate temperature was motivated by: 1) a very high difference in the grain boundary and lattice diffusion coefficient values at moderate temperatures and 2) higher grain growth at elevated temperatures. Grain growth of the nanocrystalline materials at high temperatures limits their use for high temperature applications. However, it was shown recently that addition of Zr to Fe-Cr based alloys prevents grain growth of these materials [120,121] and therefore such alloys with small amount of Zr (i.e., Fe-Cr-Zr alloys) will be ideal for investigation of oxidation resistance in the temperature range of 600-800°C.

Grain size of Fe-Cr alloys (used for the investigation of the effect of nanocrystalline structure on oxidation resistance) was limited to 54 (±4) nm which could be further decreased with the recent advancements in the sample preparation techniques such as one recently developed by Gupta et al [122] where an artefact free FeCrNi alloy with a grain size less than 10 nm was produced by in-situ consolidation technique. Further investigations on such alloys with grain size below 10 nm will demonstrate pronounced effect of triple points and grain boundaries and it may be possible to develop stainless steels with further improved oxidation resistance but less Cr content.

Improved oxidation resistance of nanocrystalline Fe-Cr or Ni-Cr-Al alloys have been attributed to the greater Cr and/or Al enrichment of the oxide scale (i.e., change in chemical composition of the oxide scale) due to faster diffusion of Cr and/or Al. However, physical properties of oxide scale, which are very important in determining the oxidation resistance of an alloy, have attracted only a little research attention. Investigation of the physical properties (grain size, morphology, crystallographic details etc.) of the oxide scale formed on the nanocrystalline alloys will further help in understanding the effect of nanocrystalline structure on the oxidation resistance of an alloy.

8. Concluding remarks

Nanocrystalline materials are being investigated due to their unique properties. More generally, development of materials resistant to environmental degradation is not the main focus of nanocrystalline metals research to date, but it seems possible that nanocrystalline metallic materials may lead to a substantial increment in oxidation resistance; caused by promoted oxide scale formation, improved adherence and reduced spallation tendency of the oxide scale. Nanocrystalline Fe-Cr and M-Cr-Al alloys have demonstrated improved oxidation resistance and present potential to be used for high temperature applications in future. More fundamental investigations are required to fully characterise the oxidation phenomenon and underlying principles for nanocrystalline materials.

9. References

[1] H. Gleiter, Progress in Materials Science, 33 (1989) 223.
[2] G. Palumbo, S. J. Thorpe, K. T. Aust, Scripta Metall. Mater. 24 (1990) 2347.
[3] C. C. Koch, K.M. Yousef, R. O. Scattergood, K. L. Murty, Advanced Eng. Mater. 7 (2005) 787
[4] R. W. Siegel, NanoStructured Materials 4 (1994) 121
[5] R. Birringer, H. Gleiter, H. P. Klein, P. Marquardt, Phys. Lett. A 102 (1984) 365.
[6] M. A. Meyers, A. Mishra, D. J. Benson, Progress in Materials Science 51 (2006) 427.

[7] T. Zhu, J. Li, Progress in Materials Science 55 (2010) 710.
[8] C. C. Koch, Encyclopedia of Materials: Science and Technology (2001) 5901.
[9] C. C. Koch, Scripta Materialia, 49 (2003) 657.
[10] S. Cheng, E. Ma, Y. M. Wang, L. J. Kecskes, K. M. Youssef, C. C. Koch, U. P. Trociewitz, K. Han, Acta Materialia 53 (2005) 1521.
[11] Z. B. Wang, N. R. Tao, W. P. Tong, J. Lu, K. Lu, Acta Materilia 51 (2003), 4319.
[12] R. K. Gupta, PhD thesis, Synthesis and corrosion behaviour of nanocrystalline Fe-Cr alloys, Monash University (2010).
[13] K. D. Ralston, N. Birbilis, Corrosion 66 (7) (2010) 075005 – 1
[14] G. Meng, Y. Li, F. Wang, Electrochimica Acta 51 (2006) 4277.
[15] C. T. Kwok, F. T. Cheng, H. C. Man, W. H. Ding, Materials Letters 60 (2006) 2419.
[16] Y. Li, F. Wang, Electrochimica Acta 51 (2006) 4426.
[17] X. Y. Wang, D. Y. Li, Electrochimica Acta 47 (2002) 3939.
[18] Sh. Hassani, K. Raeissi, M. Azzi, D. Li, M. A. Golozar, J. A. Szpunar, Corrosion Science 51 (2009) 2371.
[19] Kh. M. S. Youssef, C. C. Koch, P.S. Fedkiw, Corrosion Science 46 (2004) 51.
[20] L. Wang, Y. Lin, Z. Zeng, W. Liu, Q. Xue, L. Hu, J. Zhang, Electrochimica Acta 52 (2007) 4342.
[21] H. Gleiter, Acta Mater 48 (2000) 1.
[22] J. Y. Fan, X. L. Wu, K. Paul, K. Chu, Progress in Materials Science 51 (2006) 983.
[23] T. Sourmail, Progress in Materials Science 50 (2005) 816.
[24] M. E. McHenry, M. A. Willard, D. E. Laughlin, Progress in Materials Science 44 (1999) 291.
[25] G.R. Wallwork, A.Z. Hed, Oxidation of Metals, 3 (1971) 171.
[26] G. Chen, H. Lou, Surface and Coatings Technology 123 (2000) 92.
[27] Z. Liu, W. Gao, K.L. Dahm, F. Wang, Acta Materialia 46 (1998) 1691.
[28] L. Hanyi, W. Fuhui, X. Bangjie, Z. Lixin, Oxidation of Metals, 38 (1992) 299.
[29] H. Lou, S. Zhu, F. Wang, Oxidation of Metals, 43 (1995) 317.
[30] H. Lou, F. Wang, S. Zhu, B. Xia, L. Zhang, Surface and Coatings Technology, 63 (1994) 105.
[31] W. Xu, X. Song, N. Lu, C. Huang , Acta Materialia 58, (2010) 396.
[32] C. X. wang, C. W. Yang, Materials Science and Engineering R 49 (2005) 157.
[33] P. Keblinski, S.R. Phillpot, D. Wolf, H. Gleiter, Physics Letters A 226 (1997) 205.
[34] G. Chen, H. Lou, NanoStructured Materials, 11 (1999) 637
[35] G. Chen, H. Lou, Surface and Coatings Technology 123 (2000) 92.
[36] G. Chen, H. Lou, Corrosion Science 42 (2000) 1185.
[37] R. K. Singh Raman, R. K. Gupta, Corrosion science 51 (2009) 316.
[38] R. K. Gupta, R. K. Singh Raman, C. C. Koch, Journal of Materials Science 45 (2010) 4884.
[39] R. K. Singh Raman, R. K. Gupta ,C. C. Koch, Philosophical Magazine 90 (2010) 4884.
[40] U. Köster, L. Jastrow, Materials Science and Engineering A 449-451 (2007) 57.
[41] U. Köster, D. Zander, Triwikantoro, A. Rüdiger, L. Jastrow, Scripta Materialia 44 (2001) 1649.
[42] Triwikantoro, D. Toma, M. Meuris, U. Köster , Journal of Non-Crystalline Solids 250-252 (1999) 719.
[43] K. Mondal, U.K. Chatterjee, B.S. Murty, Journal of Non-Crystalline Solids, 334-335 (2004) 544.
[44] P. Kofstad, High Temperature Corrosion, Elsevier Applied Scicnece, New York (1988).
[45] D.J. Young, *High Temperature Oxidation and Corrosion of Metals,* Elsevier, Amsterdam (2008).

[46] M.K. Hossain, Corrosion Science 19 (1979) 1031.
[47] X. Peng, J. Yan, Y. Zhou, F. Wang, Acta Materialia 53 (2005) 5079.
[48] M.D. Merz, Metallurgical and Materials Transactions A, 10 (1979) 71.
[49] F. Wang, H. Lou, W. Wu, Vacuum, 43 (1992) 752.
[50] X. Zhu, R. Birringer, U. Herr, H. Gleiter, Phys. Rev. B 35 (1987) 9085.
[51] L. D. Bianco, A. Hernando, E. Bonetti, E. Navarro, Phys. Rev. B 56 (1997) 8894.
[52] T. Haubold, R. Birringer, B. Lengeler, H. Gleiter, Phys. Lett. A 135 (1989) 461.
[53] T. Haubold, W. Krauss, H. Gleiter, Philos. Mag. Lett 63 (1991) 245.
[54] A. DiCicco, M. Berrettoni, S. Stizza, E. Bonetti, G. Cocco Phys. Rev. B 12 (1994) 386.
[55] A.D. Cicco, M. Berrettoni, S. Stizza, E. Bonetti, Physica B 208-209 (1995) 547.
[56] R. K. Islamgaliev, R. Kuzel, E.D. Obraztsova, J. Burianek, F. Chmelik, R.Z. Valiev, Mater Sci and Engineering A 249 (1998) 152.
[57] H. E. Schaefer, R. Wurschum, R. Birringer, H. Gleiter, Phys. Rev. B 38 (1988) 9545.
[58] J. Wang, D. Wolf, S. R. Phillippot, H. Gleiter, Philos. Mag. A 73 (1996) 517
[59] D. Chen, Mater Sci and Engineering A 190 (1995) 193.
[60] D. Chen, Materials Letters 21 (1994) 405.
[61] R.E. Read-Hill, Physical Metallurgy Principles, Litton Educational Publishing, Inc. 1973
[62] T. Mutschele, R. Kirchheim, Scripta materialia 21 (1987) 1101.
[63] R. Kirchheim, T. Mutschele, W. Kieninger, H. Gleiter, R. Birringer, T. D. Koble, Mater Sci and Engineering A 99 (1988) 457.
[64] H. J. Fecht, NanoStructured Materials 1 (1992) 125.
[65] H. J. Fecht, Phys. Rev. Lett 65 (1990) 610.
[66] H. J. Fecht, E. Hellstern, Z. Fu, W.L Johnson, Adv. Powd. Met 2 (1989) 111.
[67] H. J. Fecht, Materials Science and Engineering A 179-180 (1994) 491.
[68] E. Hellstern E, H. J. Fecht, Z. Fu Z, W. L. Johnson, J. appl. Phys 65 (1989) 305.
[69] G. Wallner, E. Jorra, H. Franz, J. Peisl, R. Birringer, H. Gleiter, T. Haubold. W. Petry, MRS Symp. Proc 132 (1989) 149.
[70] J. Horvath, R. Birringer, H. Gleiter, Solid State Comm 62 (1987) 319.
[71] R. Birringer, P. Zimmer, Acta Materialia 57 (2009) 1703.
[72] A. Seeger, G. S. Acta metall. 1959;7:495.
[73] D. A. Smith, V. Vitek, R.C. Pond, Acta metal 24 (1977) 475.
[74] H. J.Fros, M. F. Ashby, F. Spaepen, Scripta matallurgica 14 (1980) 1051.
[75] D. Wolf, Philos. Mag. B 69 (1989) 667.
[76] Y. H. Zhao, H. W. Sheng, K. Lu, Acta Mater 49 (2001) 265.
[77] A. Lucci, G. Riontino, M. C. Tabasso, V. G. Tamanini, Acta Metall. 26 (1978) 615.
[78] B. Gu¨ nther, A. Kupmann, H. D. Kunze, 27 (1992) 833.
[79] L. Lu, M. L. Sui, K. Lu, Acta Mater. 49 (2001) 4127
[80] A. Tscho¨ pe, R. Birringer, Acta Metall. 41 (1993) 2791.
[81] A.T. Dinsdale, Calphad 15 (1991) 317.
[82] Y. K. Huang, A. A. Menovsky, F. R. Boer, NanoStructured Materials Materials 2 (1992) 587.
[83] R. Würschum, S. Herth, U. Brossmann, Advanced Engineering Materials, 5 (2003) 365
[84] I.V. Belova, G.E. Murch, J. of physics and chemistry of solids 64 (2003) 873
[85] H. Mehrer, Diffusion in Nanocrystalline Materials, springer Series in Solid-State Sciences (2007)
[86] G. Shujiang , F. Wang, S. Zhang, Surface and Coatings Technology 167 (2003) 212.
[87] H. Y. Tong, F. G. Shi , E. J. Lavernia, Scripta Metall Mater 32 (1995) 511.
[88] W. Gao, Z. Liu, Z. Li, Advanced Materials, 13 (2001) 1001.

[89] G. Chen, H. Lou, Scripta materialia 43 (2000) 119.
[90] G. F. Chen, H. Y. Lou, Materials Letters 45 (2000) 286.
[91] L. Liu, F. Wang, Materials Letters 62 (2008) 4081.
[92] F. Wang, X. Tian, Q. Li, L. Li, X. Peng, Thin and Solid Films 516 (2008) 5740.
[93] G. Cao, L. Geng, Z. Zheng, M. Naka, Intermetallics 15 (2007) 1672.
[94] H. Z. Zheng, S. Q. Lu, X. J. Dong, D. L. Quyang, Materials Science and Engineering A 496 (2008) 524.
[95] J. E. May, S. E. Kuri, P. A. P Nascente, Mater Sci and Engineering A 428 (2006) 290.
[96] J. E. May, G. Galerie, T. P. Busquim, S. E. Kuri, Materials and Corrosion 58 (2008) 87
[97] Y. Niu, Z. Q. Cao, F. G, Farne, G. Randi, C. L. Wang, Corrosion Science 45 (2003) 1125.
[98] S. Leistikow, I. Wolf and H.J. Grabke, Werkst. Korros., 38 (1987) 556.
[99] Y. Shida, N. Ohtsuka, J. Muriama, N. Fujino and H. Fujikawa, Proc. JIMS-3, High Temp. Corros., Trans. Jap. Inst. Met., 1983, 631.
[100] H. J. Grabke, E. M. Muller-Lorenz, S. Strauss, E. Pippel, J. Woltersdorf, Oxidation of Metals, 50 (1998) 314.
[101] M. Martin, N. Lakshmi, U. Koops, H.-I. Yoo, Z. Phys. Chem. 221 (2007) 1449.
[102] G. C. Wood, Oxidation of Metals, 2 (1970)
[103] V. R. Howes, Corrosion Science, 7 (1967) 735
[104] R. Lobb, H. Evans, Metal Science 26 (1981).
[105] M. Schutz, Oxidation of Metals, 44, (1995), 29
[106] H. Hindam, D. P. Whittle, Oxidaiton of Metals, 18 (1982) 245
[107] X. Y. Zhang, M.H. Shi, C. Li, N. F. Liu, Y.M. Wei, Mater Sci and Engineering A 448 (2007) 259.
[108] O. E. Kedim, S. Paris, C. Phigini, F. Bernard, E. Gaffet, Z. A. Munir, Mater Sci and Engineering A 369 (2004) 49.
[109] W. W. Smeltzer, D. P. Whittle, J. Electrochem. Soc. 125 (1978) 1116.
[110] C. J. Wagner, J. Electrochem. Soc. 99 (1952) 369.
[111] C. J. Wagner, J. Electrochem. Soc. 103 (1956) 571.
[112] C. J. Wagner, J. Electrochem. Soc. 63 (1959) 772.
[113] X. Peng, F. Wang, Oxidation – resistant nanocrystalline coatings, Development in high-temperature corrosion and protection of materials, W. Gao, Z. Li (Eds.), CRC Press, 2008.
[114] I. Kaur, W. Gust, L. Kozma, Handbook of grain and interphase boundary diffusion data: Stuttgart: Zigler Press, (1989), 523.
[115] A. W. Bowen, G .M. Leak, Metall. Trans. 1 (1970), 1695.
[116] R. Gupta, R. K. Singh Raman, C. C. Koch, Materials Science and Engineering A 494 (2008) 253.
[117] J. G. Goedjen, D. A. Shores, Oxidation of Metals 37 (1992) 125
[118] F. Wang, Oxidation of Metals 47 (1997) 247.
[119] F.J. Humphreys, M. Hatherly, Recrystallization and related annealing phenomena, Pergamon, 1996.
[120] R. K. Gupta, R. K. Singh Raman, C. C. Koch, TMS 2008 Annual Meeting 1 (2008) 151-157.
[121] K.S. Darling, R.N. Chan, P.Z. Wong, J. E. Semones, R.O. Scattergood, C.C. Koch, Scripta Materlialia 59 (2008) 530.
[122] R. K. Gupta, K. S. Darling, R. K. Singh Raman, K. R. Ravi, C. C. Koch, B. S. Murty, R. O. Scattergood, Journal of Materials Science (2011) DOI 10.1007/s10853-011-5986-6.

Corrosion Resistance

Edited by Dr Shih

ISBN 978-953-51-0467-4

Hard cover, 472 pages

Publisher InTech

Published online 30, March, 2012

Published in print edition March, 2012

The book has covered the state-of-the-art technologies, development, and research progress of corrosion studies in a wide range of research and application fields. The authors have contributed their chapters on corrosion characterization and corrosion resistance. The applications of corrosion resistance materials will also bring great values to reader's work at different fields. In addition to traditional corrosion study, the book also contains chapters dealing with energy, fuel cell, daily life materials, corrosion study in green materials, and in semiconductor industry.

How to reference

In order to correctly reference this scholarly work, feel free to copy and paste the following:

Rajeev Kumar Gupta, Nick Birbilis and Jianqiang Zhang (2012). Oxidation Resistance of Nanocrystalline Alloys, Corrosion Resistance, Dr Shih (Ed.), ISBN: 978-953-51-0467-4, InTech, Available from: http://www.intechopen.com/books/corrosion-resistance/oxidation-resistance-of-nanocrystalline-alloys

INTECH

open science | open minds

InTech Europe

University Campus STeP Ri
Slavka Krautzeka 83/A
51000 Rijeka, Croatia
Phone: +385 (51) 770 447
Fax: +385 (51) 686 166
www.intechopen.com

InTech China

Unit 405, Office Block, Hotel Equatorial Shanghai
No.65, Yan An Road (West), Shanghai, 200040, China
中国上海市延安西路65号上海国际贵都大饭店办公楼405单元
Phone: +86-21-62489820
Fax: +86-21-62489821